Published OnlineFirst July 26, 2010; DOI: 10.1158/0008-5472.CAN-10-0790

Cancer Research

SG2285, a Novel C2-Aryl-Substituted Pyrrolobenzodiazepine Dimer Prodrug That Cross-links DNA and Exerts Highly Potent Antitumor Activity

John A. Hartley[1,2], Anzu Hamaguchi[1], Marissa Coffils[1], Christopher R.H. Martin[1], Marie Suggitt[1], Zhizhi Chen[3], Stephen J. Gregson[3], Luke A. Masterson[3], Arnaud C. Tiberghien[3], Janet M. Hartley[2], Christopher Pepper[4], Thet Thet Lin[4], Christopher Fegan[4], David E. Thurston[3], and Philip W. Howard[3]

Abstract

The pyrrolobenzodiazepines (PBD) are naturally occurring antitumor antibiotics, and a PBD dimer (SJG-136, SG2000) is in phase II trials. Many potent PBDs contain a C2-*endo-exo* unsaturated motif associated with the pyrrolo C-ring. The novel compound SG2202 is a PBD dimer containing this motif. SG2285 is a water-soluble prodrug of SG2202 in which two bisulfite groups inactivate the PBD N10-C11 imines. Once the bisulfites are eliminated, the imine moieties can bind covalently in the DNA minor groove, forming an interstrand cross-link. The mean *in vitro* cytotoxic potency of SG2285 against human tumor cell lines is GI_{50} 20 pmol/L. SG2285 is highly efficient at producing DNA interstrand cross-links in cells, but they form more slowly than those produced by SG2202. Cellular sensitivity to SG2285 was primarily dependent on ERCC1 and homologous recombination repair. In primary B-cell chronic lymphocytic leukemia samples, the mean LD_{50} was significantly lower than in normal age-matched B and T lymphocytes. Antitumor activity was shown in several human tumor xenograft models, including ovarian, non–small cell lung, prostate, pancreatic, and melanoma, with cures obtained in the latter model with a single dose. Further, in an advanced-stage colon model, SG2285 administered either as a single dose, or in two repeat dose schedules, was superior to irinotecan. Our findings define SG2285 as a highly active cytotoxic compound with antitumor properties desirable for further development. *Cancer Res; 70(17); 6849–58. ©2010 AACR.*

Introduction

The pyrrolo[2,1-*c*][1,4]benzodiazepines (PBD) are a family of naturally occurring antitumor antibiotics produced by *Streptomyces* species (1). The PBD monomers, which include anthramycin and sibiromycin, exert their biological activity by binding in the minor groove of DNA with a selectivity for 5′-purine-G-purine sequences, forming a covalent bond to the exocyclic amino group of the guanine base (2). PBD dimers have been designed and synthesized by joining two monomer PBD units together through their C8-positions through a flexible linker (3–7). This has resulted in molecules capable of recognizing longer sequences of DNA (e.g., 5′-purine-GATC-pyrimidine; see Supplementary Material Section S1) and producing highly cytotoxic, nondistorting DNA interstrand cross-links in the DNA minor groove (8–11). One such dimer, SJG-136 (SG2000; Fig. 1A), was shown to have significant *in vitro* and *in vivo* antitumor activity (11, 12). It has recently completed phase I clinical trials in the United Kingdom (through Cancer Research UK; ref. 13) and in the United States (through National Cancer Institute; refs. 14, 15), and is about to enter phase II studies against both solid tumors and hematologic malignancies.

Many of the most potent naturally occurring PBD monomers have *endo-exo* unsaturation at the C2 position. Synthetic PBD monomers that retain this motif have established that C2 unsaturation enhances *in vitro* potency (16). This finding has now been applied to PBD dimers with the synthesis of SG2202 (ref. 17; Fig. 1A) where two PBD monomer units, which retain the *endo-exo* unsaturation motif in the form of a C2-aryl substituent conjugated to a 2,3 double bond, are joined through their C8/C8′ positions through a propyldioxy linker. This molecule had significantly greater *in vitro* cytotoxicity (17) compared with the C2-unsaturated parent molecule (DSB-120; ref. 8) or with SJG-136 (11). The additional C2/C2′-aryl substituents, however, lowered water solubility to a level that made further development of this compound challenging.

Authors' Affiliations: [1]Spirogen Ltd., UCL Cancer Institute; [2]CR-UK Drug-DNA Interactions Research Group, UCL Cancer Institute; [3]Spirogen Ltd., The School of Pharmacy, London, United Kingdom and [4]Department of Haematology, Cardiff University, Cardiff, United Kingdom

Note: Supplementary data for this article are available at Cancer Research Online (http://cancerres.aacrjournals.org/).

Corresponding Author: John A. Hartley, UCL Cancer Institute, University College London, Paul O'Gorman Building, 72 Huntley Street, London WC1E 6BT, United Kingdom. Phone: 44-20-7679-6055; Fax: 44-20-7679-6925; E-mail: john.hartley@ucl.ac.uk.

doi: 10.1158/0008-5472.CAN-10-0790

©2010 American Association for Cancer Research.

Downloaded from cancerres.aacrjournals.org on April 15, 2017. © 2010 American Association for Cancer Research.

Published OnlineFirst July 26, 2010; DOI: 10.1158/0008-5472.CAN-10-0790

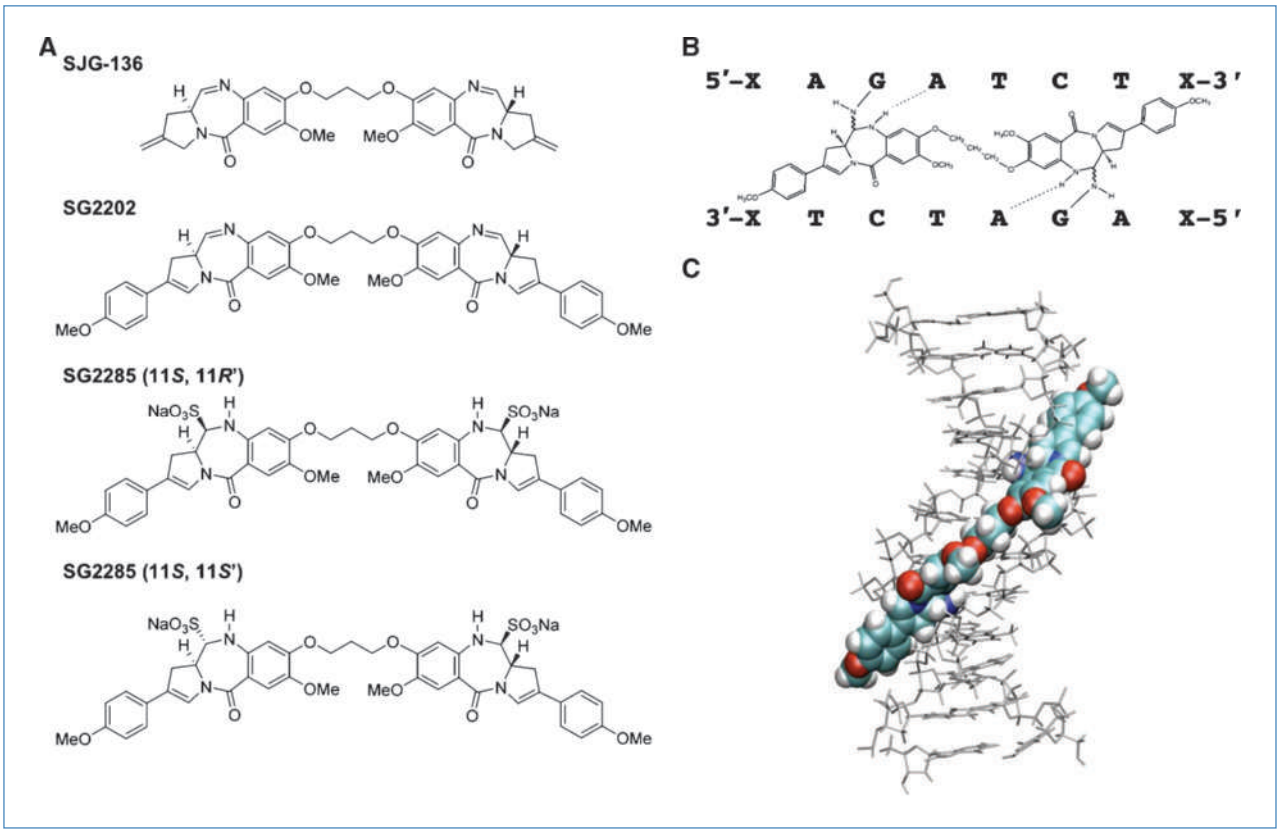

Figure 1. A, structures of SJG-136 (SG2000), SG2202, and SG2285. SG2285 is shown in the 11*S*,11′*R* and 11*S*,11*S*′ diastereomeric forms. B, scheme of SG2202 binding across 8 bp in the DNA sequence 5′-XAGATCTX-3′, forming a DNA interstrand cross-link between guanine N2 groups spanning 4 bp. C, molecular model of SG2202 binding in the DNA minor groove.

Therefore, SG2202 was converted into the C11/C11′ bisulfite adduct resulting in SG2285 (Fig. 1A; ref. 17), whereby the two bisulfite groups inactivate the N10-C11 imines of the PBD units. The prodrug exists in two predominant diastereomer forms, 11*S*,11′*R* and 11*S*,11*S*′ (Fig. 1A). Once the bisulfite groups are eliminated to produce SG2202, the two PBD imine moieties are able to bind covalently in the minor groove of DNA to the N2 positions of guanine on opposite strands of DNA to form an interstrand cross-link (Fig. 1B). SG2285 is freely water soluble and stable in aqueous conditions, retaining the *in vitro* potency of SG2202 (17). Using plasmid DNA in an agarose gel electrophoresis assay, SG2285 was found to be a highly efficient DNA interstrand cross-linking agent (17). Cross-links, however, formed more slowly than those produced by the parent molecule SG2202, reaching a peak at 2 hours for SG2202 and >18 hours for SG2285, confirming that it behaves as a prodrug.

The current study documents the *in vitro* activity of SG2285 and confirms its DNA interstrand cross-linking ability in human tumor cells. Potent activity in primary B-cell chronic lymphocytic leukemia (B-CLL; both from untreated and previously treated patients) and apoptosis induction through the intrinsic pathway are shown. In addition, potent antitumor activity is shown against a wide range of *in vivo* human solid tumor xenograft models using different dosing schedules, providing a clear rationale for further preclinical development of this novel agent.

Materials and Methods

Drugs

SG2202 and prodrug SG2285 were synthesized as previously described (17). Different batches of SG2285 containing different 11*S*,11′*R* and 11*S*,11*S*′ diastereomeric ratios were used in the current study. The ratios of 11*S*,11*S*′ to 11*S*,11′*R* for batches 2 to 5 are 1:1.87, 1:5.1, 26.5:1, and 1:9, respectively. The ratio for batch 1 was not determined.

Cell lines

All human tumor cell lines were obtained between 2003 and 2008 from the American Type Culture Collection (ATCC) or the European Collection of Cell Cultures, with the exception of LOX-IMVI and OVCAR-5, which were obtained in 2004 from the Developmental Therapeutics Program, National Cancer Institute.

The Chinese hamster ovary (CHO) AA8, UV23, UV47, UV61, and UV96 cell lines were obtained in 1998 from Dr. M. Stefanini (Istituto di Genetica Biochemica et Evoluzionistica, Pavia, Italy). V79, irs1, irs1SF, CHO-K1, and xrs5 cell lines were kindly provided in 1998 by Prof. J. Thacker (MRC Radiation and

Downloaded from cancerres.aacrjournals.org on April 15, 2017. © 2010 American Association for Cancer Research.

Published OnlineFirst July 26, 2010; DOI: 10.1158/0008-5472.CAN-10-0790

Genome Stability Unit, Harwell, United Kingdom). UV135 was obtained in 1998 from ATCC (no. CRL-1867).

All cell lines were kept at low passage, returning to original frozen stocks every 3 to 6 months, and tested regularly for *Mycoplasma*. The lines have not been reauthenticated since receipt.

Growth inhibition assays

For growth inhibition assays in human tumor cell lines, a 190-μL cell suspension was added to each well of a 96-well plate (hematologic lines at 5×10^4 cells/mL; all other lines at 1×10^4 cells/mL). Following drug addition, plates were incubated for four control cell doublings. Following incubation (with the exception of OVCAR-5 and HT29 cells), Alamar blue, which stains living cells, was added to each well to a final concentration of 1 μmol/L. For OVCAR-5 and HT29, MTT solution to a final concentration of 1.5 μmol/L was added to each well. Plates were then incubated for a further 4 hours, with the exception of U266B1 cells (5 hours) and HCT-8 cells (2 hours) at 37°C. Plates were read using an Envision plate reader, data were analyzed using GraphPad Prism, and GI_{50} values were obtained.

Studies in CHO cells were performed using the sulforhodamine B (SRB) assay as previously described (18).

Measurement of DNA interstrand cross-linking in cells using the single-cell gel electrophoresis (comet) assay

Exponentially growing DU145 cells were plated onto 2 × 6-well plates at 3×10^4/mL (2 mL/well) and incubated at 37°C overnight to allow the cells to adhere. The following day, the medium was removed and replaced with serum-free medium containing SG2285 at 1 nmol/L. The plates were then incubated at 37°C and cells were harvested at 0, 4, 8, 16, 24, and 32 hours. The cells were stored at −80°C until assayed for cross-linking using the modified single-cell gel electrophoresis (comet) assay as previously described (19, 20).

Comets were analyzed using a Nikon inverted fluorescent microscope and Kinetic Imaging software (KOMET version 4). The tail moments (TM) of 25 cells per slide were measured, and the mean tail moment of duplicate slides was calculated. The mean resultant TM (Res TM) for each dose was calculated as TM of irradiated cells − TM of unirradiated cells. The percentage decrease in TM was calculated by the following equation:

$$\%\ \text{decrease in TM} = [1 - (\text{Res TM of drug treated}/\text{Res TM control})] \times 100$$

Studies in B-CLL

Peripheral blood samples from 20 patients with B-CLL were obtained with the patients' informed consent. B-CLL was defined by clinical criteria as well as cellular morphology and the coexpression of CD19 and CD5 in lymphocytes simultaneously displaying restriction of light-chain rearrangement. None of the previously treated patients ($n = 10$) had received therapy for at least 2 months before this study.

Freshly isolated peripheral blood lymphocytes from B-CLL patients and normal age-matched controls as well as acute myelogenous leukemia cell lines (1×10^6/mL) were cultured in RPMI medium (Invitrogen) supplemented with 100 units/mL penicillin, 100 μg/mL streptomycin, and 10% fetal calf serum. Cells were incubated at 37°C in a humidified 5% carbon dioxide atmosphere in the presence of SG2285 (10^{-10}–10^{-7} mol/L) for time points up to 48 hours. Cells were harvested by centrifugation and then resuspended in 195 μL of calcium-rich buffer. Subsequently, 5 μL of Annexin V (Caltag Medsystems) was added to the cell suspension and cells were incubated in the dark for 10 minutes before washing. Cells were finally resuspended in 190 μL of calcium-rich buffer together with 10 μL of propidium iodide. Apoptosis was assessed by dual-color immunofluorescent flow cytometry.

To measure SG2285-induced caspase-3 activation, cells were harvested by centrifugation and labeled with CD19 APC-conjugated antibody. Subsequently, the cells were incubated for 1 hour at 37°C in the presence of the PhiPhiLux G_1D_2 substrate (Calbiochem), which contains two fluorophores separated by a quenching linker sequence that is cleaved by active caspase-3. Once cleaved, the resulting products fluoresce green and can be quantified using flow cytometry. In additional experiments, the caspase-8 inhibitor Z-IETD-FMK or the caspase-9 inhibitor Z-LEHD-FMK (Cambridge Bioscience) were added to SG2285-treated cell cultures (final concentration 2 μmol/L) to determine whether either of these inhibitors was able to abrogate the apoptotic effects of SG2285 in CLL cells.

Data were evaluated using the Student's t test or Mann-Whitney test, and correlation coefficients were calculated from least-squares linear regression plots. Drug sensitivity was evaluated using nonlinear regression and line of best-fit analysis of the sigmoidal dose-response curves. All statistical analyses were performed using GraphPad Prism 3.0 software.

***In vivo* studies**

LOXIMVI melanoma and OVCAR-5 ovarian tumors. United Kingdom Coordinating Committee on Cancer Research guidelines for the welfare of animals in experimental neoplasia were adhered to throughout the study.

Tumor fragments of less than 3 mm were implanted subcutaneously into the left or right flanks of the mice, and tumor growth was monitored as the relative tumor volume (RTV). Tumor volume was calculated using the formula tumor volume = $(w^2 \times l)/2$, where w is the width and l the length of the tumor. RTV was calculated using the formula RTV = tumor volume day n/tumor volume day 0. Animals were sorted into treatment groups with mean tumor volumes of 64 mm^3.

SG2285 was administered intravenously (i.v.) as a single dose, in volumes of 0.1 mL per 10 g body weight. Control groups received vehicle only. Percentage tumor growth delay (%TGD) was calculated using the formula %TGD = [time (days) taken to reach end point (treatment group) − time (days) taken to reach end point (control group)]/time (days) taken to reach end point (control group) × 100. The end point was defined as the tumor reaching 17 mm in length. Treatment outcome was evaluated by %TGD and complete regression (CR).

Downloaded from cancerres.aacrjournals.org on April 15, 2017. © 2010 American Association for Cancer Research.

Published OnlineFirst July 26, 2010; DOI: 10.1158/0008-5472.CAN-10-0790

Advanced LS174T colon and SKOV-3 ovarian tumors. LS174T xenografts were initiated from tumors maintained in *nu/nu* mice. SK-OV-3 xenografts were initiated from tumors maintained in severe combined immunodeficiency (SCID) mice. Tumor fragments of 1 mm were implanted subcutaneously into the right flanks of test mice (*nu/nu* for LS174T and SCID for SK-OV-3). The Association for Assessment and Accreditation of Laboratory Animal Care guidelines for animal care and use were adhered to throughout the study. Animals were sorted into treatment groups with mean tumor volumes of 323 to 326 mm^3 (LS174T) and 99.9 to 100 mm^3 (SK-OV-3). Compound in 5% dimethylacetamide (DMA)/95% physiologic saline was administered at various dosing regimens, in volumes of 0.1 mL per 10 g body weight. For LS174T, one group received irinotecan intraperitoneally (i.p.) weekly (qwk) × 3. Control groups received vehicle only. The end point was defined as the tumors reaching 1,500 mm^3 or 69 days for LS174T and 2,000 mm^3 or 79/120 days for SK-OV-3. Treatment outcome was evaluated by %TGD and CR.

LS174T colon, A549 non–small cell lung carcinoma, PC3 prostate, and Bx-PC-3 pancreatic tumors. LS174T, PC3, and Bx-PC-3 xenografts were initiated from tumors maintained in *nu/nu* mice. A549 xenografts were initiated from cultured cells maintained in Kaighn's modified Ham's F12 medium supplemented with 10% fetal bovine serum, 100 units/mL penicillin, 100 μg/mL streptomycin sulfate, 25 μg/mL gentamicin, 2 mmol/L glutamine, and 1 mmol/L sodium pyruvate. Tumor fragments of 1 mm were implanted subcutaneously into the right flanks of test mice. For A549 xenografts, cells were harvested during log phase and resuspended in 50% Matrigel matrix (BD Biosciences) at 5×10^7 cells/mL. Each mouse was injected subcutaneously in the right flank with 1×10^7 cells (0.2-mL cell suspension).

Animals were sorted into treatment groups with mean tumor volumes of 99 to 100 mm^3 (LS174T), 128 to 130 mm^3 (A549), 106 to 107 mm^3 (PC3), and 105 to 107 mm^3 (Bx-PC-3). SG2285 in 33% propylene glycol/5% dextrose was administered at various dosing regimens, in volumes of 0.1 mL per 10 g body weight. For LS174T, one group received irinotecan at 100 mg/kg (i.p.) qwk × 3 and one group received 5-fluorouracil (5-FU) at 100 mg/kg, i.p. qwk × 3. For A549, one group received docetaxel at 30 mg/kg, i.v. every 4 days (q4d) × 3. For PC3, one group received paclitaxel at 30 mg/kg i.v. every other day (qod) × 5 and one group received cisplatin at 10 mg/kg i.p. qwk × 3. For Bx-PC-3, one group received paclitaxel at 30 mg/kg i.v. qod × 5. Control groups received vehicle only. The end point was defined as the tumor reaching 2,000 mm^3 in the control group or 26 days (LS174T), 29 days (A549), and 30 days (Bx-PC-3). For PC3, the study was terminated at 30 days. Treatment outcome was evaluated by % tumor growth inhibition (% TGI) and partial regression (PR). %TGI was calculated using the formula $\%TGI = [(\text{median final tumor volume}_{control} - \text{median final tumor volume}_{treated})/\text{median final tumor volume}_{control})] \times 100$. An agent that produced at least 60% TGI was considered to be potentially therapeutically active. PR was indicated by tumor volumes 50% or less than the volume at day 1 of treatment.

Results

SG2285 is the C11/C11′ bisulfite adduct prodrug of SG2202 that exists in two main diastereomeric forms, 11*S*,11′*R* and 11*S*,11*S*′ (Fig. 1A). The active drug spans 8 bp in the minor groove of DNA (Fig. 1C), forming interstrand cross-links between guanine N2 positions spanning 4 bp as depicted in Fig. 1B.

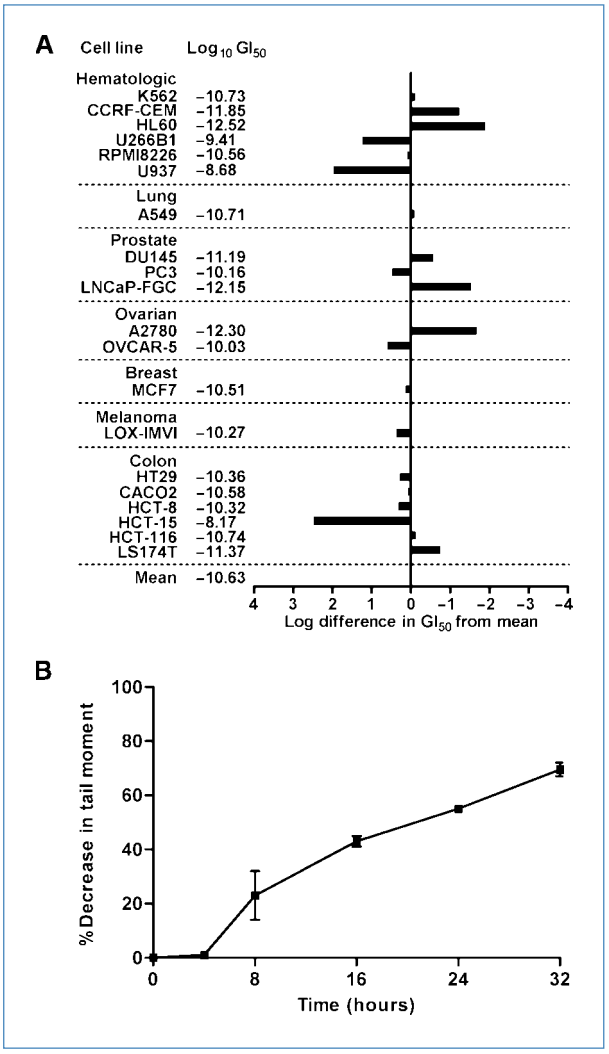

Figure 2. A, averaged mean graphs for the cytotoxicity of SG2285 against a panel of human tumor cell lines. The figure provides a graphic and tabular listing of the molar drug concentrations (log units) conferring 50% net growth inhibition (GI_{50}) for each cell line. The response of each cell line relative to the mean of all cell line responses is depicted by a horizontal bar extending either to the right (more sensitive) or to the left (less sensitive) of the mean (vertical line). The length of each bar is proportional to the cell line sensitivity relative to the mean. B, DNA interstrand cross-link formation in the human prostate cancer cell line DU-145 following treatment with 1 nmol/L SG2285. Cross-linking, expressed as the % decrease in tail moment compared with irradiated control non–drug-treated cells, was determined using the single-cell gel electrophoresis (comet) assay. Data are the mean ± SD of three independent experiments (individual experimental data are shown in Supplementary Material Section S4).

Downloaded from cancerres.aacrjournals.org on April 15, 2017. © 2010 American Association for Cancer Research.

Published OnlineFirst July 26, 2010; DOI: 10.1158/0008-5472.CAN-10-0790

Table 1. GI_{50} values for SG2285 in CHO wild-type and DNA repair–defective mutant cell lines

Cell line	Parent	Defective gene	Repair pathway	GI_{50} ± SEM (nmol/L)	S.R.
AA8	—	—	—	2.17 ± 1.17	—
UV23	AA8	*XPB*	NER	1.83 ± 0.17	1.2
UV47	AA8	*XPF*	NER	0.70 ± 0.40	3.1
UV61	AA8	*CSB*	NER	0.73 ± 0.15	3.0
UV96	AA8	*ERCC1*	NER	0.18 ± 0.04	12.1
UV135	AA8	*XPG*	NER	0.67 ± 0.15	3.2
irs1SF	AA8	*XRCC3*	HRR	0.20 ± 0.10	10.9
V79	—	—	—	3.17 ± 0.17	—
irs1	V79	*XRCC2*	HRR	0.19 ± 0.08	16.7
CHO-K1	—	—	—	0.23 ± 0.06	—
xrs5	CHO-K1	*XRCC5*	NHEJ	0.52 ± 0.39	0.4

Abbreviations: S.R., sensitivity ratio compared with wild-type; HRR, homologous recombination repair; NHEJ, nonhomologous end joining.

Activity of SG2285 *in vitro*

The *in vitro* activity of SG2285 was determined following continuous exposure in a panel of human tumor cell lines (Fig. 2A). The average GI_{50} across the panel was 20 pmol/L, range 0.3 pmol/L (HL-60) to 68 nmol/L (HCT-15). These data confirm the potent *in vitro* activity of SG2285 against both hematologic and solid tumor cell lines. In addition, the 10^4 range in GI_{50} values among the cell lines suggests that this agent confers a multilog, differential effect upon cell lines rather than exerting a nonspecific cytotoxicity. (For a comparison with other DNA cross-linking agents, see Supplementary Material Section S2, Table S1.)

The activity of SG2285 was also determined in a panel of CHO cell lines with defined defects in specific DNA repair pathways (Table 1). Cell lines defective in the nucleotide excision repair (NER) genes *XPB, XPG, XPF*, and *CSB* showed a modest increase in sensitivity (1.2- to 3.2-fold) over wild-type cells. Cells defective in the nonhomologous end joining (NHEJ) Ku 70 subunit (XRCC5) showed no increased sensitivity. In contrast, cells defective in the NER factor ERCC1 showed a 12.1-fold increased sensitivity to SG2285. In addition, cells defective in the RAD51 paralogues XRCC2 and XRCC3 were highly sensitive to SG2285, with 16.7- and 10.9-fold increased sensitivities, respectively. These data suggest that cellular sensitivity of the minor groove cross-linking agent SG2285 is dependent on ERCC1 and homologous recombination repair.

DNA interstrand cross-linking by SG2285 in cells

We have previously shown SG2285 to efficiently cross-link naked DNA (17), with the cross-links forming more slowly than with SG2202. DNA interstrand cross-linking was determined in the human prostate cancer cell line DU145 treated with 1 nmol/L SG2285 using the single-cell gel electrophoresis (comet) assay (Fig. 2B). Cross-links form slowly, with none evident in the initial 4 hours. A significant level of cross-linking was observed at 8 hours, which was still increasing at 32 hours. This is in contrast to other PBD dimers such as SJG-136 in which cross-links form rapidly in cells, with the majority forming within the first few hours of exposure (11). These data are therefore consistent with SG2285 acting as a prodrug, slowly releasing the highly potent cross-linking agent SG2202.

Study of SG2285 in primary B-CLL cells

In vitro drug sensitivity was measured in 20 primary B-CLL samples using the Annexin V/propidium iodide assay, and LD_{50} values were calculated. Apoptosis was induced in all 20 patient samples following exposure to SG2285 with a mean LD_{50} value (±SD) of 8.3 (±3.4) × 10^{-9} mol/L (Fig. 3A) and LD_{90} value of 4.6 (±2.4) × 10^{-8} mol/L. Normal B and T lymphocytes from 10 age-matched controls showed higher LD_{50} values than the B-CLL cells ($P < 0.0001$ and $P < 0.0001$, respectively; Fig. 3A). This difference was not observed with the cross-linking agent chlorambucil, for which the normal cells were found to be more sensitive (Fig. 3A)

The development of drug resistance in B-CLL is associated with previous treatment and is often pleiotropic in nature (21). In this study, we compared SG2285 LD_{50} values between previously treated ($n = 10$) and untreated ($n = 10$) patient groups (Fig. 3B). There was a trend toward increased resistance to SG2285 in the previously treated group, but this did not reach statistical significance ($P = 0.07$), whereas the increase was significant with chlorambucil ($P = 0.003$).

Aliquots of B-CLL cells were exposed to 5 or 10 nmol/L SG2285 for up to 72 hours. Apoptosis induction was dose-related and increased significantly between 36 and 48 hours, and was still increasing at 72 hours (Fig. 3C). DNA interstrand cross-linking in B-CLL cells was evaluated at 2 nmol/L. Consistent with the apoptosis induction, and the data in Fig. 2B, cross-links formed slowly and were only evident after 8 hours, and still increasing at 48 hours (see Supplementary Material Section S3; Fig. S1).

To elucidate the exact caspase activation pathway that SG2285 uses in B-CLL cell killing, a series of experiments were performed using caspase inhibitors to evaluate their

Downloaded from cancerres.aacrjournals.org on April 15, 2017. © 2010 American Association for Cancer Research.

Published OnlineFirst July 26, 2010; DOI: 10.1158/0008-5472.CAN-10-0790

ability to block SG2285-induced apoptosis (Fig. 3D). The pan caspase inhibitor Z-VAD.fmk at a concentration of 2 μmol/L significantly inhibited the cytotoxic effects of SG2285. The caspase-9 inhibitor (LEHD.fmk) also caused a reduction in SG2285-induced apoptosis at a final concentration of 2 μmol/L; however, the caspase-8 inhibitor (IETD.fmk) had little cytoprotective effect as shown in Fig. 3D. Therefore, SG2285 induces apoptosis through the intrinsic apoptotic pathway.

Antitumor activity of SG2285 *in vivo*

The antitumor activity of SG2285 was evaluated in a range of human tumor xenograft models using different i.v. dosing schedules. Representative experiments are shown in Fig. 4, and data from all experiments are summarized in Tables 2 and 3. In an early-stage melanoma LOX-IMVI, which was previously shown to be sensitive to SJG-136 (11), a single administration of SG2285 at 3 mg/kg gave seven of seven tumor-free survivors at the end of the study period (day 68; Fig. 4A; Table 2). A further study gave eight of eight tumor-free survivors at day 86, with single doses of 1.5 and 0.75 mg/kg giving six of eight and four of eight tumor-free survivors, respectively. Activity was also observed in the ovarian OVCAR-5 model following a single administration of 3 mg/kg (% TGD = 59), although no tumor-free survivors or CRs were seen in this model (Table 2).

In an advanced LS174T colon model (mean tumor volume >300 mm^3 at start of treatment), SG2285 was also effective following a single administration of 4 mg/kg (Fig. 4B), giving %TGD of 138 (Table 2). Improved efficacy was observed using repeated schedules of 1.5 mg/kg q4d × 3 or 0.8 mg/kg daily (qd) × 5 (Fig. 4B), giving %TGD values of 219 and 202, respectively. In this model, SG2285 was considerably more efficacious than irinotecan at a standard dose of 100 mg/kg i.p. qwk × 3 (%TGD = 54; Fig. 4B). In the SKOV-3 ovarian cancer model, SG2285 was highly effective using a q4d × 3 schedule at doses of 0.5, 0.25, and 0.1 mg/kg (Fig. 4C), giving %TGD values of 325, 309, and 325, respectively (Table 2). At the top dose, eight of nine of the animals were still alive at the end of the experiment (120 days). In contrast, with the standard agent cisplatin at 8 mg/kg qwk × 3, all animals had to be sacrificed by day 92 (Fig. 4C). Further experiments in this model confirmed the potent activity of SG2285 using both a q4d × 3 schedule and a qd × 5 schedule with tumor-free survivors observed at 0.375 and 1.5 mg/kg (q4d × 3) and 0.4 and 0.8 mg/kg (qd × 5; Table 2). Comparison in this model between different batches of drug containing different 11*S*,11′*R* and 11S,11*S*′ diastereomer ratios ranging from 1:1.87 (batch 2) to 26.5:1 (batch 4) confirmed activity in all cases (Table 2).

Significant activity was also observed in a series of shorter-duration *in vivo* experiments (26–30 days) using 100 mm^3 tumors (Table 3). SG2285 at 0.85 and 1 mg/kg qd4 × 3 was superior to irinotecan (100 mg/kg qwk × 3 i.p.) and 5-FU (100 mg/kg qwk × 3 i.p.) in the LS174T colon model. SG2285 (1 mg/kg q4d × 3), although producing a significant tumor growth delay, was less active than docetaxel (30 mg/kg qwk × 3) in the non–small cell lung cancer model A549 (%TGI 63 and 89, respectively). In the PC3 prostate model, SG2285 gave 5 of 10 and 4 of 10 PRs at 0.75 q4d × 4 and 1.0 mg/kg q4d × 3, respectively, which was superior to cisplatin (10 mg/kg qwk × 3 i.p., no PRs) but less active than paclitaxel (30 mg/kg qod × 5, 8 of 10 PRs). Finally, SG2285 gave PRs in the Bx-PC-3 prostate cancer model, whereas none was seen with paclitaxel.

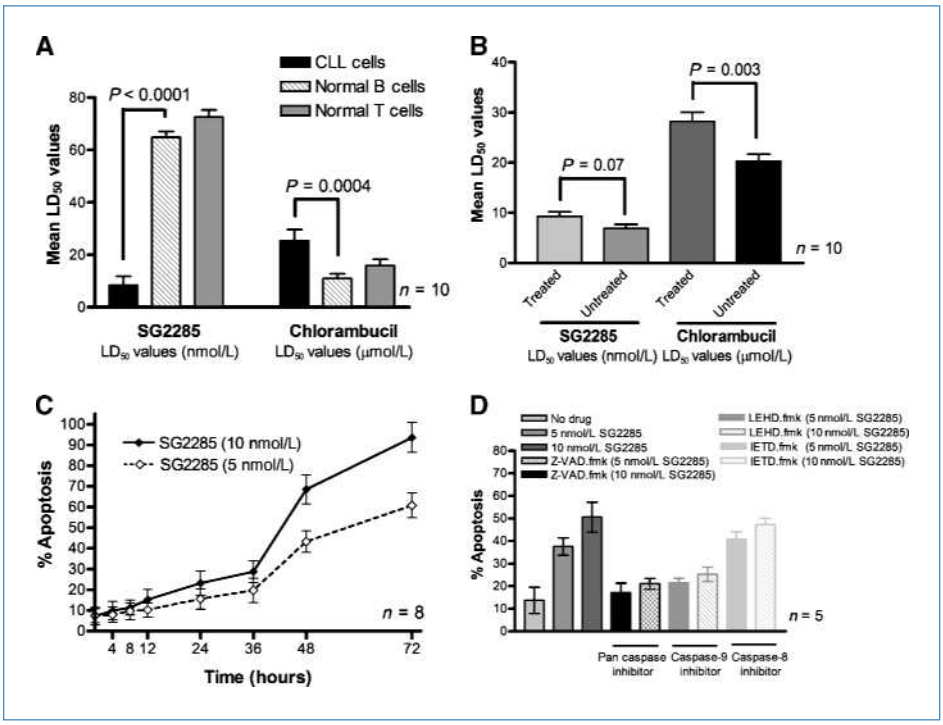

Figure 3. A, cytotoxicity of SG2285 or chlorambucil expressed as LD_{50} values (±SD) derived from *in vitro* primary B-CLL samples from 20 patients and B- and T-lymphocyte subsets from 10 normal age-matched control samples. Data are mean ± SD. B, comparison of LD_{50} values (mean ± SD) for SG2285 or chlorambucil in samples derived from previously treated (n = 10) and untreated (n = 10) CLL patients. C, kinetics of apoptosis induction in primary B-CLL cells treated with 5 and 10 nmol/L SG2285. D, effect of caspase inhibitors on apoptosis in B-CLL cells following exposure to SG2285 for 48 hours. Results are the mean (±SD) of three separate experiments.

Downloaded from cancerres.aacrjournals.org on April 15, 2017. © 2010 American Association for Cancer Research.

Published OnlineFirst July 26, 2010; DOI: 10.1158/0008-5472.CAN-10-0790

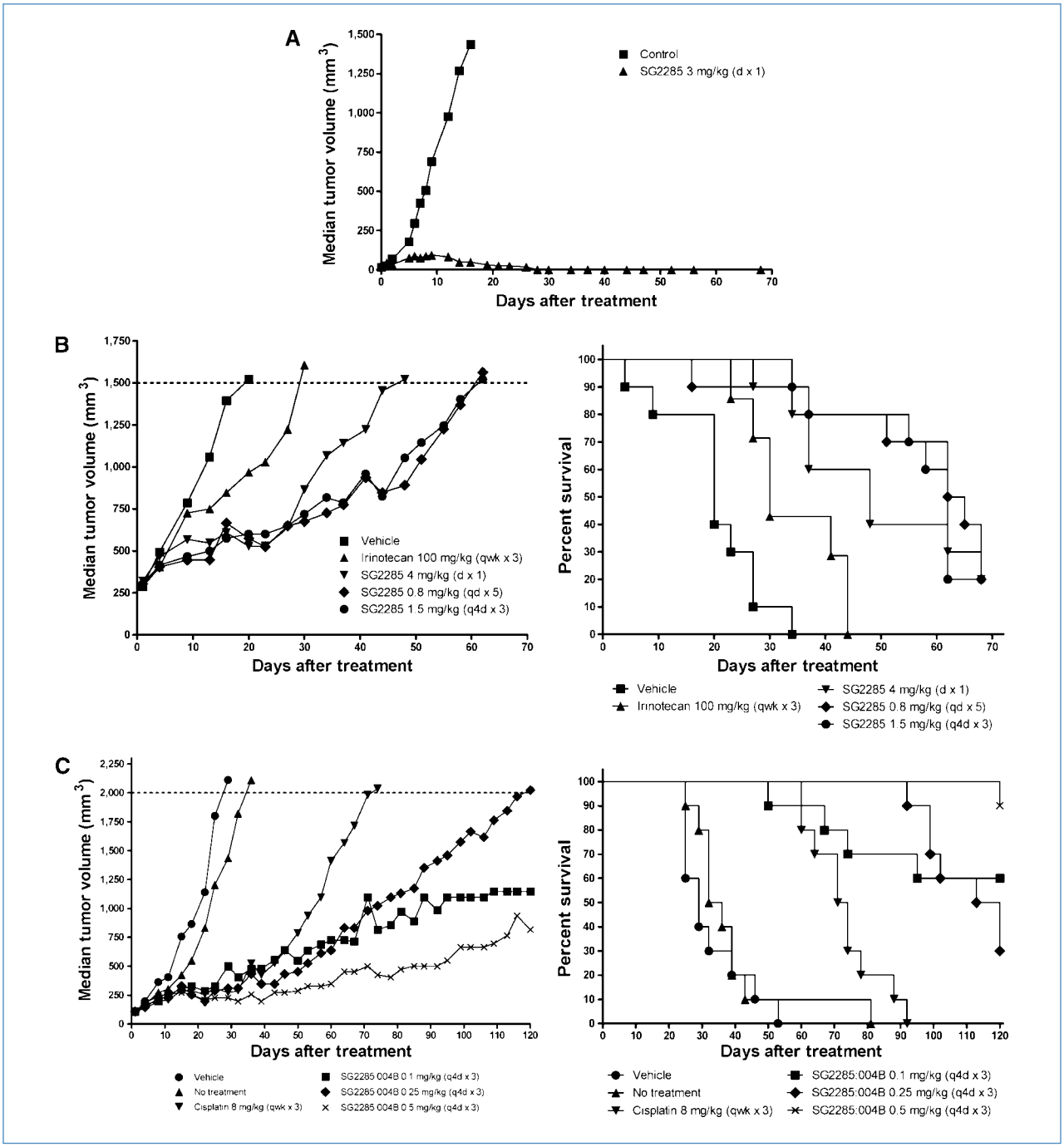

Figure 4. Representative *in vivo* human tumor xenograft experiments following treatment with SG2285. A, tumor growth curves for single i.v. exposure to LOX-IMVI human melanoma. Data are from seven animals in each group resulting in seven of seven tumor-free survivors at day 68. B, tumor growth curves (left) and Kaplan-Meier plots (right) for the advanced LS174T human colon tumor model following treatment with SG2285 at three different schedules (4 mg/kg d × 1, 0.8 mg/kg qd × 5, 1.5 mg/kg q4d × 3). Irinotecan (100 mg/kg qwk × 3) is included for comparison. Data are from 10 animals per group. C, tumor growth curves (left) and Kaplan-Meier plots (right) for the SKOV-3 human ovarian tumor model following treatment with SG2285 q4d × 3 at 0.1, 0.25, and 0.5 mg/kg. Cisplatin (8 mg/kg qwk × 3) is included for comparison.

Discussion

SG2202 is the first example of a C2/C2′-aryl PBD dimer that has been converted to a stable, highly water soluble prodrug form (SG2285) by conversion to C11/C11′-bisulfite diastereomers. SG2285 retains the *in vitro* potency of SG2202 (17). The formation of DNA interstrand cross-links by SG2285 is significantly delayed compared with SG2202

Downloaded from cancerres.aacrjournals.org on April 15, 2017. © 2010 American Association for Cancer Research.

Published OnlineFirst July 26, 2010; DOI: 10.1158/0008-5472.CAN-10-0790

both in naked DNA (17) and in intact cells. In both cases, a similar level of cross-linking is eventually achieved, consistent with SG2285 acting as a prodrug and releasing the bisulfite groups to provide a slow conversion to the active PBD dimer SG2202.

SG2285 is more potent *in vitro* than SJG-136, the first PBD dimer to enter clinical trials. For example, the mean GI_{50} in the panel of human tumor cell lines (Fig. 2) was 20 pmol/L compared with 7.4 nmol/L for SJG-136 in the NCI 60 cell line panel (11). Consistent with this increased potency is the ~50-fold lower concentration of SG2285 required to produce an equivalent level of DNA interstrand cross-linking in cells.

The data obtained in the panel of DNA repair–defective CHO mutants indicated that sensitivity to SG2285 was primarily dependent on ERCC1 and homologous recombination (XRCC2 and XRCC3; refs. 22–25). With conventional cross-linking agents such as nitrogen mustards and platinum drugs, the XPF-ERCC1–specific nuclease has been shown to play a critical role in repair or "unhooking" of interstrand cross-links both in cell-free systems and in cells (26–28). We have previously shown in the same panel of cell lines that sensitivity to SJG-136 was increased 7.5-fold in both XPF- and ERCC1-defective cells (18). Interestingly, for SG2285, the level of sensitivity in ERCC1 (12.1-fold) was much higher than for XPF (3.1-fold), suggesting a greater dependence on ERCC1. This has not been observed previously for other cross-linking agents. Consistent with other cross-linking agents, however, including SJG-136, is the highly increased sensitivity (11- and 17-fold) of SG2285 in XRCC2 and XRCC3 cells, confirming the importance of homologous recombination repair in the processing of unhooked and resectioned interstrand cross-links (18, 27–29).

Potent *in vitro* activity was also confirmed in primary B-CLL samples with an LD_{50} value more than 2 logs lower than fludarabine, the current treatment choice for this condition, and lower than SJG-136 (30). Importantly, SG2285 exhibited significant differential apoptotic activity (by the intrinsic apoptotic pathway) between normal B and T lymphocytes, and B-CLL cells. In addition, leukemic cells isolated from previously treated patients were not more resistant to SG2285 compared with those isolated from treatment-naïve patients. Taken together, these data indicate that SG2285 might be a useful option for the treatment of this hematologic malignancy, which remains incurable with a median survival for advanced-stage patients of only 3 years (31).

SG2285 was found to be a highly active antitumor agent *in vivo*, with activity observed in all models tested. CRs and tumor-free survivors were observed in the LOX-IMVI melanoma and SKOV-3 ovarian models, and tumor regressions in the PC3 prostate and Bx-PC-3 pancreatic models, representing hard-to-treat cancers, following single cycles of treatment. Significant and long-lasting tumor growth delays were

Table 2. Summary of *in vivo* data for SG2285 in human tumor xenograft models LOX-IMVI (melanoma), advanced LS174T (colon), OVCAR-5 (ovarian), and SKOV-3 (ovarian)

Model	Tumor type	Dose (mg/kg) (batch)	Schedule (i.v.)	Duration (d)	%TGD*	CR (TFS)
LOX-IMVI	Melanoma	3 (1)	d × 1	68	n/a	7/7 (7/7)
LOX-IMVI	Melanoma	3 (1)	d × 1	86	n/a	8/8 (8/8)
		1.5 (1)	d × 1	86	6/8 (6/8)	
		0.75 (1)	d × 1	86	4/8 (4/8)	
Advanced LS174T†	Colon	4 (2)	d × 1	69	138	—
		1.5 (2)	q4d × 3	69	219	—
		0.8 (2)	qd × 5	69	202	—
OVCAR-5	Ovarian	3 (1)	d × 1	56	59	—
SKOV-3	Ovarian	0.8 (2)	qd × 5	79	168	1/8 (1/8)
		0.4 (2)	qd × 5	79	77	1/8 (1/8)
		0.2 (2)	qd × 5	79	63	—
		1.5 (2)	q4d × 3	79	229	1/8 (1/8)
		0.75 (2)	q4d × 3	79	129	—
		0.375 (2)	q4d × 3	79	85	1/8 (1/8)
SKOV-3	Ovarian	0.1 (3)	q4d × 3	120	325	—
		0.25 (3)	q4d × 3	120	309	—
		0.5 (3)	q4d × 3	120	325	—
		0.2 (4)	q4d × 3	120	156	1/8 (1/8)
		0.5 (4)	q4d × 3	120	180	—
		1.0 (4)	q4d × 3	120	248	—

Abbreviations: TFS, tumor-free survivors (i.e., CRs at the end of study); n/a, not applicable; d x 1, single administration.
*%TGD = $[(T - C)/C] \times 100$.
†Irinotecan (100 mg/kg i.p. qwk × 3) gave %TGD of 54 in this experiment (see Fig. 4B).

Downloaded from cancerres.aacrjournals.org on April 15, 2017. © 2010 American Association for Cancer Research.

Published OnlineFirst July 26, 2010; DOI: 10.1158/0008-5472.CAN-10-0790

Table 3. Summary of *in vivo* data for SG2285 and appropriate standard agents in human tumor xenograft models LS174T (colon), A549 (non–small cell lung), PC3 (prostate), and Bx-PC-3 (pancreatic)

Model	Drug	Dose (mg/kg) (batch)	Schedule*	Duration (d)	%TGI†	PR‡
LS174T (colon)	SG2285	0.85 (3)	q4d × 3	26	83	0
		1.0 (3)	q4d × 3	26	82	0
	Irinotecan	100	qwk × 3 (i.p.)	26	46	0
	5-FU	100	qwk × 3 (i.p.)	26	65	0
A549 (NSCLC)	SG2285	1.0 (5)	q4d × 4	29	63	0
	Docetaxel	30	qwk × 3	29	89	0
PC3 (prostate)	SG2285	0.75 (5)	q4d × 4	30	96	5/10
		1.0 (5)	q4d × 3	30	96	4/10
	Paclitaxel	30	qod × 5	30	99	8/10
	Cisplatin	10	qwk × 3 (i.p.)	30	72	0
Bx-PC-3 (pancreatic)	SG2285	1.0 (3)	q4d × 4	30	86	2/9
		1.0 (3)	q4d × 3	30	69	1/9
		1.0 (5)	q4d × 4	30	81	1/8
		1.0 (5)	q4d × 3	30	84	2/8
	Paclitaxel	30	qod × 5	30	47	0

*Drug was given i.v. unless indicated otherwise.
†%TGI = [1 − (*T*/*C*)] × 100 = % tumor growth inhibition compared with vehicle controls. TGI ≥ 60% indicates therapeutic activity.
‡Tumor volume 50% or less than its day 1 volume for three consecutive measurements.

observed in the other models tested, including an advanced LS174T colon model in which increases in life span of >40 days and superior activity to the standard drug irinotecan were achieved. Activity was observed in single i.v. and repeat dose (q4d × 3 and qd × 5) schedules. All studies tested a single cycle of treatment, and there is clearly the potential for increased activity with repeated treatment cycles. In comparison with irinotecan, it is interesting to note that both compounds covalently link to bases on opposite DNA strands with a 4-bp stagger.

The delivery of the PBD dimer SG2202 as a prodrug has resulted in an agent (SG2285) with very different cellular and animal pharmacokinetic properties to SJG-136. Interestingly, despite the active cross-linking agent SG2202 being considerably more potent than SJG-136, the maximum tolerated dose (MTD) of prodrug SG2285 in mice is ~10-fold higher than for SJG-136. In LOX-IMVI and OVCAR-5, direct comparisons can be made between SG2285 and SJG-136, and in both cases SG2285 gave superior activity. For example, under the identical conditions used for SG2285 shown in Fig. 4A, SJG-136 was highly active but produced cures in only four of eight animals at its MTD (0.3 mg/kg), whereas SG2285 cured all animals (eight of eight) at 3 mg/kg, six of eight animals at 1.5 mg/kg, and four of eight at 0.75 mg/kg. In the case of OVCAR-5, a single administration of SJG-136 at its MTD produced only a minimal growth delay, whereas SG2285 gave a significant tumor growth delay (Table 2). The data suggest that the delivery of a highly active PDB as a prodrug can result in an increased therapeutic index *in vivo*.

The diastereomeric ratio of SG2285 was found to be very sensitive to its method of synthesis, work-up, and purification. For example, one set of conditions affords almost exclusively the 11*S*,11*S*′ diastereomer (26.5:1 11*S*,11*S*′ to 11*S*,11′*R* ratio), whereas different conditions can produce a 9:1 mixture in favor of the 11*S*,11′*R* diastereomer (17). Importantly, the ratio of C11/C11′ diastereomers does not seem to influence *in vitro* cytotoxicity of SG2285 (data not shown). The present study also shows that batches of drug with 11*S*,11*S*′ to 11*S*,11′*R* ratios ranging from 26.5:1 to 1:5.1 retain potent *in vivo* antitumor activity.

In summary, SG2285 is a novel C2-aryl-substituted PBD dimer prodrug with potent activity *in vitro* against human tumor cell lines and primary B-CLL cells, and *in vivo* against a wide range of human tumors, including those difficult to treat clinically. As a result of this impressive activity, SG2285 is in preclinical development toward phase I clinical trials.

Disclosure of Potential Conflicts of Interest

SG2285 is owned by Spirogen Ltd., in which J.A. Hartley, P.W. Howard, and D.E. Thurston have equity interests.

Acknowledgments

We thank Dr. David Evans for the molecular model of SG2202 binding to DNA.

Grant Support

Spirogen Ltd. (United Kingdom); Cancer Research UK programme grant C2259/A9994 (JAH), and the UCL Experimental Cancer Medicine Centre.

The costs of publication of this article were defrayed in part by the payment of page charges. This article must therefore be hereby marked *advertisement* in accordance with 18 U.S.C. Section 1734 solely to indicate this fact.

Received 03/04/2010; revised 07/15/2010; accepted 07/15/2010; published OnlineFirst 07/24/2010.

Downloaded from cancerres.aacrjournals.org on April 15, 2017. © 2010 American Association for Cancer Research.

Published OnlineFirst July 26, 2010; DOI: 10.1158/0008-5472.CAN-10-0790

References

1. Thurston DE. Advances in the study of pyrrolo[2,1-*c*][1,4]benzodiazepine (PBD) antitumor antibiotics. In: Neidle S, Waring MJ, editors. Molecular aspects of anticancer drug-DNA interactions. London: The Macmillan Press Ltd; 1993, p. 54–88.
2. Hurley LH, Reck T, Thurston DE, et al. Pyrrolo(1,4)benzodiazepine antitumor antibiotics: relationship of DNA alkylation and sequence specificity to the biological activity of natural and synthetic compounds. Chem Res Toxicol 1988;1:258–68.
3. Bose DS, Thompson AS, Ching J, et al. Rational design of a highly efficient irreversible DNA interstrand cross-linking agent based on the pyrrolobenzodiazepine ring system. J Am Chem Soc 1992;114:4939–41.
4. Bose DS, Thompson AS, Smellie M, et al. Effect of linker length on DNA-binding affinity, cross-linking efficiency and cytotoxicity of C8-linked pyrrolobenzodiazepine dimers. J Chem Soc Chem Commun 1992;14:1518–20.
5. Thurston DE, Bose DS, Thompson AS, et al. Synthesis of sequence-selective C8-linked pyrrolo[2,1-*c*][1,4]benzodiazepine DNA interstrand crosslinking agents. J Org Chem 1996;61:8141–7.
6. Gregson SJ, Howard PW, Hartley JA, et al. Design synthesis and evaluation of a novel pyrrolobenzodiazepine DNA-interactive agent with highly efficient cross-linking ability and potent cytotoxicity. J Med Chem 2001;44:737–8.
7. Gregson SJ, Howard PW, Gullick DR, et al. Linker length modulates DNA crosslinking reactivity and potency for ether-linked C2-exo-unsaturated pyrrolo[2,1-*c*][1,4]benzodiazepine (PBD) dimers. J Med Chem 2004;47:1161–74.
8. Smellie M, Kelland LR, Thurston DE, Souhami RL, Hartley JA. Cellular pharmacology of novel C8-linked anthramycin-based sequence-selective DNA minor-groove cross-linking agents. Br J Cancer 1994;70:48–53.
9. Smellie M, Bose DS, Thompson AS, Jenkins TC, Hartley JA, Thurston DE. Sequence selective recognition of duplex DNA through covalent interstrand crosslinking: kinetic and molecular modelling studies with pyrrolobenzodiazepine (PBD) dimers. Biochemistry 2003;42:8232–9.
10. Martin C, Ellis T, McGurk CJ, et al. Sequence-selective interaction of the minor-groove interstrand cross-linking agent SJG-136 with naked and cellular DNA: footprinting and enzyme inhibition studies. Biochem 2005;44:4135–47.
11. Hartley JA, Spanswick VJ, Brooks N, et al. SJG-136 (NSC 694501), a novel rationally designed DNA minor groove interstrand cross-linking agent with potent and broad spectrum antitumor activity. Part 1: cellular pharmacology, *in vitro* and initial *in vivo* antitumor activity. Cancer Res 2004;64:6693–9.
12. Alley MC, Hollingshead MG, Pacula-Cox CM, et al. SJG-136 (NSC 694501), a novel rationally designed DNA minor groove interstrand cross-linking agent with potent and broad spectrum antitumor activity. Part 2: efficacy evaluations. Cancer Res 2004;64:6700–6.
13. Hochhauser D, Meyer T, Spanswick VJ, et al. Phase 1 study of a sequence selective minor groove DNA binding agent (SJG-136) with pharmacokinetic and pharmacodynamic measurements in patients with advanced solid tumors. Clin Cancer Res 2009;15:2140–7.
14. Puzanov I, Lee W, Berlin JD, et al. Final results of phase I and pharmacokinetic trial of SJG-136 administered on a daily ×3 schedule. Proc Am Soc Clin Oncol Ann Meet J Clin Oncol 2008;26:Abs 2512.
15. Janjigian YY, Lee W, Kris MG, et al. A phase I trial of SJG-136 (NSC694501) in advanced solid tumors. Cancer Chemother Pharmacol 2010;65:833–8.
16. Cooper N, Hagan DR, Tiberghien A, et al. Synthesis of novel C2-aryl pyrrolobenzodiazepines (PBDs) as potential antitumour agents. Chem Commun 2002;16:1764–5.
17. Howard PH, Chen Z, Gregson SJ, et al. Synthesis of a novel C2/C2′-aryl-substituted pyrrolo[2,1-*c*]-[1,4]benzodiazepine dimer prodrug with improved water solubility and reduced DNA reaction rate. Bioorganic Med Chem Lett 2009;19:6463–6.
18. Clingen PH, De Silva IU, McHugh PJ, et al. The XPF-ERCC1 endonuclease and homologous recombination contribute to the repair of minor groove DNA interstrand crosslinks in mammalian cells produced by the pyrrolo[2,1-*c*][1,4]benzodiazepine dimer SJG-136. Nucleic Acids Res 2005;33:3283–91.
19. Hartley JM, Spanswick VJ, Gander M, et al. Measurement of DNA crosslinking in patients on ifosfamide therapy using the single cell gel electrophoresis (comet) assay. Clin Cancer Res 1999;5:507–12.
20. Spanswick VJ, Hartley JM, Ward TH, Hartley JA. Measurement of drug-induced DNA interstrand crosslinking using the single cell gel electrophoresis (comet) assay. In: Brown R, Boger-Brown U, editors. Methods in molecular medicine. Vol. 28: cytotoxic drug resistance mechanisms. New York: Humana Press; 1999, p. 143–54.
21. Pepper C, Thomas A, Hidalgo de Quintana J, Davies S, Hoy T, Bentley P. Pleiotropic drug resistance in B-cell chronic lymphocytic leukaemia—the role of Bcl-2 family proteins. Leuk Res 1999;23:1007–14.
22. Cartwright R, Tambini CE, Simpson PJ, Thacker J. The XRCC2 DNA repair gene from human and mouse encodes a novel member of the recA/RAD51 family. Nucleic Acids Res 1998;26:3084–9.
23. Liu N, Lamerdin JE, Tebbs RS, et al. XRCC2 and XRCC3, new human Rad51-family members, promote chromosome stability and protect against DNA cross-links and other damages. Mol Cell 1998;1:783–93.
24. Yamada NA, Hinz JM, Kopf VL, Segalle KD, Thompson LH. XRCC3 ATPase activity is required for normal XRCC3-51C complex dynamics and homologous recombination. J Biol Chem 2004;279:23250–4.
25. Yokoyama H, Sarai N, Kagawa W, et al. Preferential binding to branched DNA strands and strand-annealing activity of the human Rad51B, Rad51C, Rad51D and Xrcc2 protein complex. Nucleic Acids Res 2004;32:2556–65.
26. Kuraoka I, Kobertz WB, Ariza RR, Biggerstaff M, Essigmann JM, Wood RD. Repair of an interstrand DNA cross-link initiated by ERCC1-XPF repair/recombination nuclease. J Biol Chem 2000;275:26632–6.
27. De Silva IU, McHugh PJ, Clingen PH, Hartley JA. Defining the roles of nucleotide excision repair and recombination in the repair of DNA interstrand cross-links in mammalian cells. Mol Cell Biol 2000;20:7980–90.
28. De Silva IU, McHugh PJ, Clingen PH, Hartley JA. Defects in interstrand cross-link uncoupling do not account for the extreme sensitivity of ERCC1 and XPF cells to cisplatin. Nucleic Acids Res 2002;30:3848–56.
29. McHugh PJ, Spanswick VJ, Hartley JA. Repair of DNA interstrand crosslinks: molecular mechanisms and clinical relevance. Lancet Oncol 2001;2:483–90.
30. Pepper CJ, Hambly RM, Fegan CD, Delavault P, Thurston DE. The novel sequence-specific DNA cross-linking agent SJG-136 (NSC 694501) has potent and selective *in vitro* cytotoxicity in human B-cell chronic lymphocytic leukemia cells with evidence of a p53-independent mechanism of cell kill. Cancer Res 2004;64:6750–5.
31. Lee JS, Dixon DO, Kantarjian HM, Keating MJ, Talpaz M. Prognosis of chronic lymphocytic leukemia: a multivariate regression analysis of 325 untreated patients. Blood 1987;69:929–36.

Downloaded from cancerres.aacrjournals.org on April 15, 2017. © 2010 American Association for Cancer Research.

Published OnlineFirst July 26, 2010; DOI: 10.1158/0008-5472.CAN-10-0790

AACR American Association for Cancer Research

Cancer Research

The Journal of Cancer Research (1916–1930) | The American Journal of Cancer (1931–1940)

SG2285, a Novel C2-Aryl-Substituted Pyrrolobenzodiazepine Dimer Prodrug That Cross-links DNA and Exerts Highly Potent Antitumor Activity

John A. Hartley, Anzu Hamaguchi, Marissa Coffils, et al.

Cancer Res 2010;70:6849-6858. Published OnlineFirst July 26, 2010.

Updated version	Access the most recent version of this article at: doi:10.1158/0008-5472.CAN-10-0790
Supplementary Material	Access the most recent supplemental material at: http://cancerres.aacrjournals.org/content/suppl/2010/07/26/0008-5472.CAN-10-0790.DC1

Cited articles	This article cites 29 articles, 13 of which you can access for free at: http://cancerres.aacrjournals.org/content/70/17/6849.full.html#ref-list-1
Citing articles	This article has been cited by 4 HighWire-hosted articles. Access the articles at: /content/70/17/6849.full.html#related-urls

E-mail alerts	Sign up to receive free email-alerts related to this article or journal.
Reprints and Subscriptions	To order reprints of this article or to subscribe to the journal, contact the AACR Publications Department at pubs@aacr.org.
Permissions	To request permission to re-use all or part of this article, contact the AACR Publications Department at permissions@aacr.org.

Downloaded from cancerres.aacrjournals.org on April 15, 2017. © 2010 American Association for Cancer Research.